

# The Impact of Altering Emission Data Precision on Compression Efficiency and Accuracy of Simulations of the Community Multiscale Air Quality Model

Michael S. Walters<sup>§,†,\*</sup> and David C. Wong<sup>§,\*</sup>

5 <sup>§</sup>Atmospheric and Environmental Systems Modeling Division, Center for Environmental Measurement and Modeling, Office of Research and Development, U.S. Environmental Protection Agency, Research Triangle Park, NC, USA

<sup>†</sup>Oak Ridge Associated Universities, Oak Ridge, TN, USA.

<sup>\*</sup>These authors contributed equally to this work.

10 *Correspondence to:* David C. Wong (wong.david-c@epa.gov)

**Abstract.** The Community Multiscale Air Quality Model (CMAQ) has been a vital tool for air quality research and management at the United States Environmental Protection Agency (U.S. EPA), and at government environmental agencies and academic institutions worldwide. CMAQ requires a significant amount of disk space to store and archive input and output files. For example, an annual simulation over the contiguous United States with horizontal grid cell spacing of 12 km requires 2–3 TB of input data and can produce anywhere from 7–45 TB of output data, depending upon modelling configuration, and desired post-processing of the output (e.g., for evaluations or graphics). After a simulation is complete, model data are archived for several years, or even decades, to ensure the replicability of conducted research. As a result, careful disk space management is essential to optimize resources and ensure the uninterrupted progress of ongoing research and applications requiring large scale, air quality modelling. Proper disk space management may include applying optimal data compression techniques that are executed on input and output files for all CMAQ simulations. There are several (not limited to) such utilities that compress files using lossless compression, such as GNU Gzip and Basic Leucine Zipper Domain (bzip2). A new approach is proposed in this study that reduces the precision of the air quality model emissions input to reduce storage requirements (after a lossless compression utility is applied) and accelerate runtime. The new approach is tested using CMAQ simulations and post-processed CMAQ output to examine the impact on the air quality model performance. In total, four simulations were conducted, and nine cases were post-processed from direct simulation output to determine disk space efficiency, runtime efficiency, and model (predictive) accuracy. Three simulations were run with emissions input containing only five, four, or three significant digits. To enhance the analysis of disk space efficiency, the output from the altered precision emissions CMAQ simulations were additionally post-processed to contain five, four, or three significant digits. The fourth, and final, simulation was run using the full precision emissions files with no alteration. Thus, in total, 13 gridded products (four simulations and nine altered-precision output cases) were analysed in this study.

Results demonstrate that the ~~altered~~altered-precision emission files reduced the disk space footprint by 6 %, 25 %, and 48 % compared to the unaltered emission files when using the bzip2 compression utility for files containing five, four, or three significant digits, respectively. Similarly, the altered output files reduced the required disk space by 19 %, 47 %, and 69 % compared to the unaltered CMAQ output files when using the bzip2 compression utility for files containing five, four, or three significant digits, respectively. For both compressed datasets, bzip2 performed better than gzip, in terms of compression size, by 5–27 % for emission data and 15–28 % for CMAQ output for files containing five, four, or three significant digits. Additionally, CMAQ runtime was reduced by 2–7 % for simulations using emission files with reduced precision data on a non-dedicated environment. Finally, the model estimated pollutant concentrations from the four simulations were compared to observed data from the U.S. EPA Air Quality System (AQS) and the Ammonia Monitoring Network (AMON). Model performance statistics were negligibly impacted (~~e.g., normalized mean bias differed by less than 0.01 % for all altered simulations and cases~~). In summary, by reducing the precision of CMAQ emissions data to five, four, or three significant digits, the simulation runtime on a non-dedicated environment was slightly reduced, disk space usage was substantially reduced, and model accuracy remained relatively unchanged compared to the base CMAQ simulation, which suggests that the precision of the emissions data could be reduced to more efficiently use computing resources while minimizing the impact on CMAQ simulations.

## 1. Introduction

The Community Multiscale Air Quality (CMAQ) model (Byun and Schere, 2006) is a sophisticated, message passing interface (MPI) based, three-dimensional Eulerian (gridded) numerical modelling system that uses scientific first principles to simulate the chemical transformation and transport of ozone, particulate matter, toxic compounds, and acid deposition.

Since the formation and transformation of chemical species are functions of complex atmospheric and chemical interactions, two primary input types are required to initialize CMAQ simulations: meteorology and emissions. First, meteorological data (such as temperature, wind, cloud formation, and precipitation rate) provide atmospheric conditions to drive CMAQ. The second required input field, which is the focal point of this study, is emissions data (i.e., emission rates from emission sources) that characterize pollutants from both man-made and naturally occurring sources.

~~The chemical transport model within~~ CMAQ model typically requires multiple emission datasets which occupy a significant amount of disk space. Although disk space is becoming progressively cheaper and more affordable, the research and computational needs are rapidly increasing and becoming more complex. For instance, the total sizes of emission and meteorological datasets are about 7.0 GB and 6.8 GB, respectively for a one-day CMAQ simulation for the contiguous U.S. with a horizontal resolution of 12 km. The total disk space size for one day of output is 20 GB (for a typical output configuration considering only surface output and neglecting extra diagnostic output). Including 3D fields and diagnostic output, however, the total output disk space size can easily be tripled. Most studies with CMAQ on this scale create at least a full year's worth of data, so aggressive disk space management ~~approaches could be justified~~ is justifiable to minimize

overall costs associated with running CMAQ. Aggressive disk space management could be a substantial cost-savings measure, regardless of whether simulations are conducted onsite (such as with a high-performance computing architecture or a Linux cluster) or by using cloud computing, where data retrievals can quickly elevate costs. Here, we propose optimizing disk space by compressing CMAQ emission datasets as one practical consideration to maximize storage capacity. If successful, this option could be extended to other input types with large disk space needs, such as meteorological data.

Compression algorithms can be described as either lossless or lossy. Lossless compression algorithms reduce disk space by replacing repeated sequences with a smaller, unique identifier. Thus, an entire dataset can be retrieved, once uncompressed, without alteration of the original dataset (hence the name, lossless). Lossy algorithms, however, in terms of numeric arrays, reduce disk space by manipulating the mantissa of ~~a single individual~~ floating point ~~numbers~~. Typically, trailing, or insignificant bits, are replaced with a sequence of zeros or ones. As a result, data is compressed at the cost of numeric inconsistencies between the original dataset and the compressed dataset.

The concept of maximizing disk space by altering netCDF datasets has been examined previously by Zender (2016) and Kouznetsov (2020). Zender (2016) created a versatile toolset that compresses data based on user specifications that are applied to the mantissa of floating-point datasets. The first notable algorithm developed by Zender (2016) is precision-trimming, which is publicly available in the netCDF operators (NCO, <http://nco.sourceforge.net/nco.html>) utility. Precision-trimming sets all non-significant bits to zero (bit shaving) which, based on analysis, produces an undesirable bias of the compressed data (Zender 2016). As a result, Zender (2016) introduced a Bit Grooming algorithm (default algorithm in NCO) that shaves (to zero) and sets (to one) the least significant bits of consecutive values. Despite the additional toolset, Kouznetsov (2021) found substantial artifacts, or numeric inconsistencies, in multipoint statistics caused by Bit Grooming. Due to the suboptimal results, Kouznetsov (2021) developed and evaluated multiple lossy compression algorithms with respect to NCO's available toolsets from Zender (2016). Kouznetsov (2021) created a round and halfshave lossy compression algorithm which both doubled compression accuracy by rounding the mantissa to the nearest value that has 0 tail bits and by setting all tail bits to zero except for the most significant bit which gets set to one (Kouznetsov, 2021).

Excluding analyses conducted on datasets via lossy compression algorithms, the authors are unaware of any studies that have been conducted on the compression efficiency on floating-point datasets with respect to  $n$  significant digits. Additionally, Zender (2016) and Kouznetsov (2021) did not conduct evaluations regarding the impact of ~~altered~~~~altered-precision~~ datasets on numeric simulations. In this study, netCDF datasets will be ~~altered-reduced-precision~~ and compressed to explore compression efficiency, and the resultant ~~altered-reduced-precision~~ datasets will be used to run CMAQ simulations to quantify the impacts on runtime and on model accuracy as a result of dataset manipulation via a lossy compression algorithm. This study proceeds as ~~such~~~~follows~~: in Sect. 2, a description of the methodology will be provided, followed by results in Sect. 3, then the conclusions in Sect. 4.

## 2. Methodology

95 All input and output files in this study are 32-bit, binary, netCDF files which inherently contain seven or eight significant digits at most. To perform this study, we created a simple tool written in Fortran to truncate floating-point data in netCDF files by keeping  $n$  significant digits which are normalized in scientific notation. Table 1 shows several examples of this numerical manipulation.

100 We applied this tool to alter the precision of two different datasets (input emission and CMAQ model output) by keeping  $n$  significant digits.

For this study, CMAQ v5.3.1 (USEPA 2019, Appel et. al. 2021) was run with 459 columns, 299 rows, and 35 vertical layers with a horizontal grid-scale resolution of 12 km (Fig. 1.a). Emission input files consist of two area sources and nine point sources (hourly). The area source emission files contain 57 and 62 variables, and the point source files contain anywhere from 54 to 58 variables (containing one vertical layer). Ten CMAQ output files (nine of them are hourly) were generated in this study: Three output files were generated for simulation restart purposes (SOILOUT, CGRID which contains only one hour data, and MEDIA), two files contained average (APMDIAG and ACONC) and hourly (CONC) species concentrations, three files held wet deposition (WETDEP1; 140 variables), dry deposition (DRYDEP; 174 variables), and deposition velocity (DEPV; 104 variables) output, and lastly, the final file contained biogenic emission diagnostic output (B3GTS) using 12 km grid spacing.

105 this study: Three output files were generated for simulation restart purposes (SOILOUT, CGRID which contains only one hour data, and MEDIA), two files contained average (APMDIAG and ACONC) and hourly (CONC) species concentrations, three files held wet deposition (WETDEP1; 140 variables), dry deposition (DRYDEP; 174 variables), and deposition velocity (DEPV; 104 variables) output, and lastly, the final file contained biogenic emission diagnostic output (B3GTS) using 12 km grid spacing.

110 In total, wWe conducted four annual CMAQ simulations for 2016: one with un~~altered~~altered emission data (simulation *orig*) and three with ~~altered~~altered-precision emissions data by setting  $n$  to five (*A05*), four (*A04*), and three (*A03*) for all emission input files (gridded\_no\_rwc, gridded\_rwc, ptnonipm, ptegu, ptagfire, ptfire, ptfire\_othna, pt\_oilgas, cmv\_c3\_12, cmv\_c1c2\_12, and othpt) utilized by CMAQ for this study. On the output side, direct CMAQ output (ACONC, APMDIAG, DRYDEP, and WETDEP1) from the *A05*, *A04*, and *A03* (in which *A0n* signifies an ~~altered~~altered simulation which utilized

115 ~~altered~~altered-precision emissions data to  $n$  significant digits) simulations was similarly ~~altered~~altered to possess five, four, or three significant digits (denoted as *FX05*, *FX04*, and *FX03*, respectively in which *FX0n* signifies an ~~altered~~altered-precision case which was post-processed by an *A0n* simulation's CMAQ output). Emission input and CMAQ output data were then compressed separately by gzip (GNU Gzip, <https://www.gnu.org/software/gzip>) and bzip2 (<https://www.sourceware.org/bzip2>) for all simulations and cases to determine compression efficiency in terms of the reduction of disk space. In summary, there are four separate simulations (called *orig* or abbreviated as *A0n*) and nine additional, ~~altered~~altered-precision output cases (abbreviated as *FX0n*). For example, a CMAQ simulation that was run with emissions data that was processed with  $n$  equals five significant digits, then post-processed to possess three significant digits, is denoted as *A05FX03* (see Table 2 for ~~more a~~ full list of simulations and cases).

120 Simulated numeric, or predictive, accuracy was analyzed against concentrations of particulate matter with diameter less than

125 2.5  $\mu\text{m}$  ( $\text{PM}_{2.5}$ ), ozone ( $\text{O}_3$ ), ammonia ( $\text{NH}_3$ ), the wet deposition rates of sodium (Na), ammonium ( $\text{NH}_4$ ), chlorine (Cl), nitrate ( $\text{NO}_3$ ), sulfate ( $\text{SO}_4$ ), and the dry deposition rate of  $\text{O}_3$  for all simulations and cases.  $\text{PM}_{2.5}$  and  $\text{O}_3$  were evaluated at in

situ stations from the United States Environmental Protection Agency's (U.S. EPA) Air Quality System (AQS; Fig. 1.b) dataset. NH<sub>3</sub> was evaluated at in situ stations utilizing observations from the Ammonia Monitoring Network (AMON; Fig. 1.c). Hourly observations of O<sub>3</sub> were processed to calculate the maximum 8-hour daily average concentrations (MDA8) and paired in space and time with calculated MDA8 O<sub>3</sub> from post-processed CMAQ output. Likewise, ~~daily averaged PM<sub>2.5</sub> observations and two-week averaged NH<sub>3</sub> observations were used to evaluate CMAQ~~ daily averaged NH<sub>3</sub> and PM<sub>2.5</sub> observations were used to evaluate CMAQ. Observed values are paired with the volume-average pollutant estimate from CMAQ's surface layer's grid cell containing the air quality monitoring site (i.e., nearest neighbor). Statistical metrics were also calculated by pairing gridded values from the *orig* simulation (considered observed values) and the ~~altered~~ precision simulations and cases (considered the predicted values). Tabulated statistical metrics for grid-grid pairing was computed by taking the mean of ~~specific~~ hourly, statistical metrics.

Typical statistical metrics including mean bias (MB), correlation coefficient (r), root-mean-square-error (RMSE) and normalized mean bias (NMB) are used to evaluate all chemical species in this analysis at different temporal intervals and for different pairing methodologies (either grid-point or grid-grid) which includes regional stratification (based on regions from Fig. 1.a) for several figures. The utilized statistical metrics are denoted below in Eq. (1) through Eq. (4).

$$MB = \frac{1}{N} \cdot \sum_{i=1}^N (Y_i - X_i), \quad (1)$$

$$r = \frac{1}{N-1} \cdot \frac{\sum_{i=1}^N ((X_i - \bar{X})(Y_i - \bar{Y}))}{\sigma_X \cdot \sigma_Y}, \quad (2)$$

$$RMSE = \sqrt{\frac{\sum_{i=1}^N (Y_i - X_i)^2}{N}}, \quad (3)$$

$$NMB = \frac{\sum_{i=1}^N (Y_i - X_i)}{\sum_{i=1}^N (X_i)} \cdot 100\%, \quad (4)$$

~~Where N is the total number of observed and predicted pairs, X is the observed value, Y is predicted value, σ is the sample standard deviation of a distribution, and the overbars in Eq. (2) refers to the sample mean of a distribution. Where N is the total number of observed and predicted pairs, X is the observed value, Y is predicted value, σ is the standard deviation of a distribution, and the overbars in Eq. (2) refers to the mean of a distribution.~~

Although many compression toolsets exist and optimization is dependent on multiple factors (Kryukov et al., 2020), gzip and bzip2 are the most public, reliable, and widely used compressors. Both utilities are lossless compression algorithms which are available for Linux users. In terms of functionality, gzip uses a compression algorithm called Deflate (Deutsch, 1996) which reduces sequences of datasets by incorporating a combination of LZ77 dictionary coding (Ziv and Lempel, 1977) and Huffman entropy coding (Huffman, 1952). In comparison, bzip2 uses the Burrows-Wheeler (Burrows and Wheeler, 1994) algorithm which sorts all possible rotations of an input lexically and forms an output by concatenating the last character from the sorted list ~~chronologically reduces sequences of datasets by processing sequences through multiple layers of compression algorithms~~. In terms of compression ratio, bzip2 is notably better than gzip, however, with respect to compression speed,

gzip is significantly faster than bzip2. Due to their availability and efficiency, both gzip and bzip2 are utilized in this study (default settings).

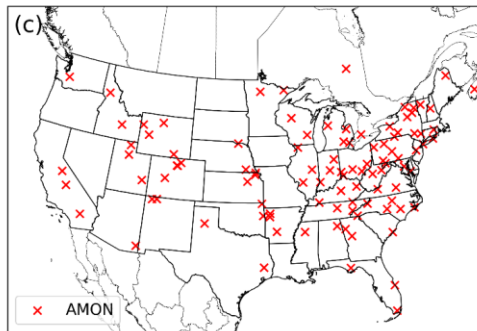
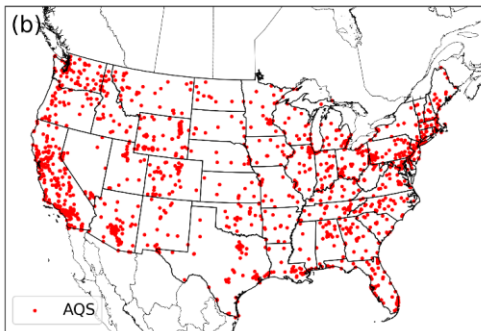
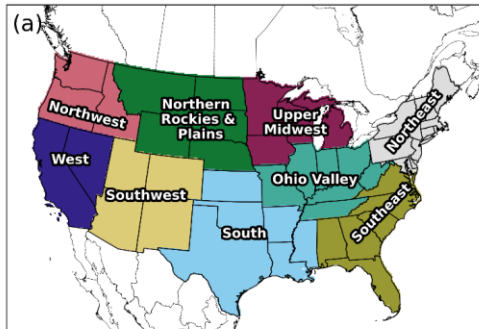
**Table 1: Multiple Examples of precision-reducing transformations of floating points from their original forms (first column) to their altered-precision forms (second to fourth column).**

Original (orig)	Altered 5 (A05)	Altered 4 (A04)	Altered 3 (A03)
0.005666635	0.0056666	0.005667	0.00567
$3.437405 \times 10^{-6}$	$3.4374 \times 10^{-6}$	$3.437 \times 10^{-6}$	$3.44 \times 10^{-6}$
0.0005319762	0.00053198	0.000532	0.000532
$3.437 \times 10^{-6}$	$3.437 \times 10^{-6}$	$3.437 \times 10^{-6}$	$3.44 \times 10^{-6}$
<u>100150.0</u>	<u>100150.0</u>	<u>100200.0</u>	<u>100000.0</u>

**Table 2: Setup of all simulations (*orig*, A05, A04, and A03) and cases analyzed in this study.**

<u>Unaltered</u> Emissions Data		<u>Altered-Precision</u> Emissions Data					
a)	Simulation: <i>orig</i>	b)	Simulation: A05	c)	Simulation: A04	d)	Simulation: A03
<u>Altered-precision</u> CMAQ Output							
	e)	Case: A05FX05	h)	Case: A04FX05	k)	Case: A03FX05	
	f)	Case: A05FX04	i)	Case: A04FX04	l)	Case: A03FX04	
	g)	Case: A05FX03	j)	Case: A04FX03	m)	Case: A03FX03	

160



165

Figure 1: Regions for spatial and temporal stratification (a), AQS stations (b), and AMON stations (c) for the proceeding evaluation.

### 3. Results

#### 3.1. Data Storage

170

CMAQ input and output data are stored for future analyses and to ensure the reproducibility of modeling studies which demands a tremendous amount of disk space for input and output files. Therefore, we propose to ease the disk space burden by utilizing efficient compression algorithms. For this section of the analysis, two popular, reliable, and efficient compression utilities, gzip and bzip2, were utilized to determine compression efficiency with respect to emission input (emissions mentioned in section 2.) files and CMAQ output (mentioned in section 2. including CGRID, CONC, and SOILOUT) files. Both compression utilities were applied daily to compress emission input and CMAQ output files throughout the entirety of [the 2016 simulation](#) (Fig. 2).

175

The gzip compression utility reduced the file sizes, ~~on by an average by~~ of 1 %, 5 %, and 21 %; ~~This translates into~~ about 5 GB, 26 GB, and 111 GB, ~~actual difference between compressed orig case and relative reduction in file size of~~ the compressed ~~daily~~ A05, A04, and A03 emissions datasets for ~~the entire year of~~ 2016, respectively, ~~compared to the orig case.~~

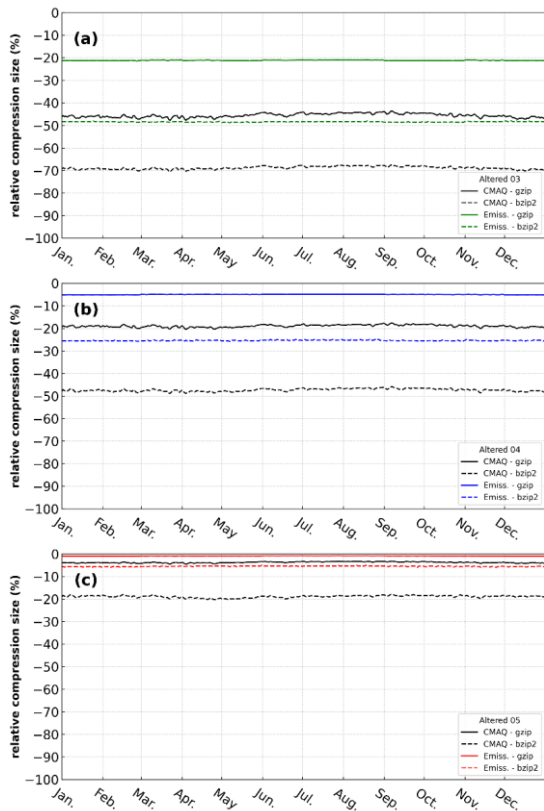
Formatted: Font: Italic

180 The reduction in file size (using gzip) was more substantial when applied to ~~direct-reduced-precision~~ CMAQ output, with an average reduction in file size of 4 %, 19 %, and ~~647~~ %; ~~This means~~ about 167 GB, 839 GB, and 2016 GB ~~actual difference between orig case and for~~ FXA05, FXA04, and FXA03, respectively ~~for the entire year.~~ With the bzip2 utility, the reduction in magnitude is much larger than with gzip, with an average reduction of file size equal to 6 %, 25 %, and 48 %; ~~or~~ ~~(actual differences are about~~ 27 GB, 126 GB, and 241 GB, respectively for A05, A04, and A03 emissions files and 19 %, 47  
185 %, and 69 % ~~(actual differences are about,~~ or 856 GB, 2142 GB, and 3115 GB, respectively, for the compressed CMAQ output. Thus, bzip2 is found to be a more effective tool than gzip by roughly 5 %, 20 %, and 27 % for emission data and 15 %, 28 % and 23 % for CMAQ output, for ~~A05, A04, and A03~~ reduced-precision by keeping 5, 4, and 3 significant digits ~~(preprocessed-reduced-precision emission and postprocessed-reduced-precision output data), respectively.~~

Formatted: Font: Italic

Formatted: Font: Not Italic





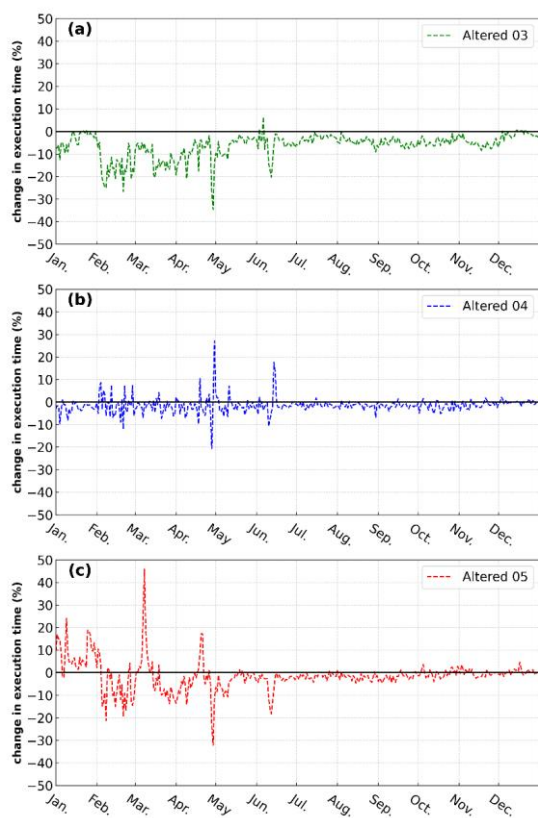
190 Figure 2: Relative compression size of two utilities, gzip (solid line) and bzip2 (dotted line), on daily emission files (labelled as Emiss.) and direct CMAQ output (labelled as CMAQ) for 2016 with ~~adigit (via the FX program) set to reduced-precision settings;~~ 5, 4, and 3 (labelled as Altered 05, Altered 04, and Altered 03, respectively). Negative values indicate better compression efficiency.

### 3.2. Runtime

195 We examined daily runtime (captured by an MPI function called MPI\_WTIME) for CMAQ using emissions data prepared with truncations of *A05*, *A04*, and *A03* compared with running CMAQ with un~~altered~~*altered* (*orig*) emissions data (Fig. 3). Even though the simulations were not performed in a dedicated environment (results are not entirely consistent due to the allocation of resources when the simulations were initialized), the daily runtimes for *A05*, *A04*, and *A03* were consistently lower than the runtime of the *orig* simulation in most of the days. The total runtimes for the *A05*, *A04*, and *A03* simulations

were 3.13, 2.94, and 12.84 hours faster than the *orig* case (2 %, 2 %, and 7 %, respectively of relative reduction of runtime).

There are two possible explanations for such behavior: First, during the execution of each case, CMAQ competed for I/O resources with other tasks on the system. As a result, an I/O bottleneck could explain spikes in relative run-time on certain simulation days (Fig. 3). Second, a change in emission input (due to the reduced-precision emission data) could alter the pathway for the aerosol dynamics calculation.



205 **Figure 3:** Relative daily run time with respect to different adjusted emission input for the A03, A04, and A05 simulations for 2016.

### 3.3. Accuracy

The accuracy of each case is first examined grid-to-point between modeled output and in situ observations (Fig. 1; AQS and AMON) for all available modeled-model-measurement pairs throughout 2016. In general, to gauge the accuracy of CMAQ, bulk statistical metrics of bias, NMB, r, and RMSE have been provided in Table 3 for the *orig* simulation. To compare bulk statistical metrics to the *orig* simulation, the absolute difference in bias, RMSE, minima (minimum difference between all model and observation pairs), and maxima was calculated with respect to the altered simulations and cases for daily PM<sub>2.5</sub>, MDA8 O<sub>3</sub>, and two-week averaged NH<sub>3</sub>. Overall, negligible differences are apparent (Fig. 4). Resultantly, each case performed with negligible differences when compared against the *orig* case in terms of statistical parameters provided for daily PM<sub>2.5</sub>, MDA8 O<sub>3</sub>, and daily NH<sub>3</sub> (Tables 3–5). For example, the maximum absolute, bulk statistical difference between the *orig* simulation and the altered cases and simulations bulk statistic range of NMB for daily PM<sub>2.5</sub>, MDA8 O<sub>3</sub>, and two-week averaged daily NH<sub>3</sub> amongst all cases is  $1.845 \times 10^{-3} \%$ ,  $1.088 \times 10^{-4} \%$ , and  $7.873 \times 10^{-4} \%$  did not exceed  $1.4 \times 10^{-4}$ ,  $3.6 \times 10^{-5}$ ,  $1.1 \times 10^{-1}$ , and  $5.3 \times 10^{-3} \mu\text{g m}^{-3}$  or ppb for bias, RMSE, minima, and maxima, respectively. Therefore, differences in terms of maximum absolute, bulk statistical differences are quite small amongst the unaltered simulation (*orig*) and the altered simulations and cases at most, simulations deviated from one another by  $1.845 \times 10^{-3} \%$  (for PM<sub>2.5</sub>) utilizing bulk statistical metrics of NMB. Similarly, the range for all statistical metrics (Table 3–5) are quite small.

Bulk statistical results with respect to in situ observations and compared to the *orig* simulation (Fig. 4)(Tables 3–5) are encouraging; differences are small ignoring regional or temporal stratification. To determine if statistical results fluctuate spatially (by region) and or temporally (by season), RMSE was computed for 9 different sub-regions (regions are portrayed in Fig. 1) across the United States for four seasons (Winter, Spring, Summer, and Fall) from the mentioned observation and model pairs. Each region's RMSE was stacked together, by simulation and case, and plotted as 'accumulated RMSE' by species. Likewise, results have are negligible differences for daily PM<sub>2.5</sub>, MDA8 O<sub>3</sub>, and daily NH<sub>3</sub> two-week averaged NH<sub>3</sub>, respectively (Fig. 45) for all regional and temporal stratifications and for all simulations and cases.

Results indicate that all simulations and cases have negligible differences in terms of bulk statistical metrics across the U.S. and considering regional and temporal stratifications. To identify small scale, temporal discrepancies, absolute bias ( $|Y_i - X_i|$ ) was calculated for all daily PM<sub>2.5</sub>, MDA8 O<sub>3</sub>, and daily NH<sub>3</sub> observation and model pairs for all simulations and cases. Similarly, results suggest little impact in terms of range of maximum and minimum absolute bias. In fact, the ranges of maximum absolute bias for daily PM<sub>2.5</sub>, MDA8 O<sub>3</sub>, and daily NH<sub>3</sub>, computed from the biases of each simulation and case, are  $0.16 \mu\text{g m}^{-3}$ ,  $0.13 \text{ ppb}$ , and  $0.001 \mu\text{g m}^{-3}$  respectively (Table 6). In contrast, the 24 hour fine particle limit for PM<sub>2.5</sub> exposure is  $35 \mu\text{g m}^{-3}$  and the 8 hour exposure limit for O<sub>3</sub> is  $70 \text{ ppb}$  (U.S. EPA Criteria Pollutants, <https://www.epa.gov/criteria-air-pollutants/naaqs-table>). Thus, the ranges of maximum absolute bias for PM<sub>2.5</sub> and O<sub>3</sub> do not exceed air quality criteria ( $0.16 \mu\text{g m}^{-3} < 35 \mu\text{g m}^{-3}$  and  $0.13 \text{ ppb} < 70 \text{ ppb}$ ) which suggests the differences in simulations and cases are negligible.

Formatted: Subscript

Statistical results conducted on in situ observations were redone (methodologically) at the grid level for hourly PM<sub>2.5</sub>, O<sub>3</sub>, and NH<sub>3</sub>, using the *orig* simulation (as the observed field) with respect to the ~~altered~~altered-precision simulations and cases (predicted fields). RMSE was first calculated for all hourly grid–grid pairs for PM<sub>2.5</sub>, O<sub>3</sub>, and NH<sub>3</sub>. Only cells that are within each region (Fig. 1.a), within the contiguous US, were used to calculate hourly RMSE for all available regional pairs. Next, the average, hourly RMSE was calculated for each season and region based on spatial and temporal masking using the regions portrayed in Fig. 1.a. All stratifications were grouped together as accumulative, stacked bar plots for different seasons by simulation or case. Although differences are evident (Fig. 56), the scale of such differences is quite small. For example, the total accumulative RMSE for PM<sub>2.5</sub>, O<sub>3</sub>, and NH<sub>3</sub> (sum of all region’s RMSE) did not exceed 0.044 μg m<sup>-3</sup>, 0.34 ppbV, and 0.054 ppbV, respectively for all cases and for all seasons.

Additionally, the maximum absolute bias for all grid cells was determined spatially between the *orig* simulation and the altered simulations and cases throughout 2016 for PM<sub>2.5</sub>, O<sub>3</sub>, and NH<sub>3</sub> from gridded, hourly (CMAQ) output. For PM<sub>2.5</sub>, all simulations and cases performed similarly in which no visual differences are apparent (Fig. 67). For O<sub>3</sub> (Fig. 78) and NH<sub>3</sub> (Fig. 89), however, the differences become relatively large for cases *n* = 3. In fact, for both species, spatial and magnitude error visibly increases with fewer significant digits (simulations and cases). For example, maximum absolute bias is largest for the *A03* simulations and even worse for the *FX03* ~~altered~~altered-precision cases ignoring the artifact of error across the Northeast U.S. for O<sub>3</sub> for the *A05* simulations and cases (induced by the *A05* simulation). The maximum absolute bias ranges, found by taking the range of all ~~altered~~altered-precision cases, for PM<sub>2.5</sub>, O<sub>3</sub>, and NH<sub>3</sub> are 46.77 μg m<sup>-3</sup>, 0.4265 ppbV, and 18.78 ppbV, respectively (Table 74). The minimum absolute bias ranges for PM<sub>2.5</sub>, O<sub>3</sub>, and NH<sub>3</sub> are 5.573 μg m<sup>-3</sup>, 0.5091 ppbV, 9.778 ppbV (Table 74), respectively. Based on range, error can potentially be quite large compared to the statistics provided in Fig. 56, however, large-scale error is not persistent based on the small accumulated RMSE for all regions grouped by CMAQ simulation and case (Fig. 56). For example, for PM<sub>2.5</sub>, the maximum positive bias was (roughly) between 41 and 51 μg m<sup>-3</sup> for the *FX03* cases (Table 4). Upon further investigation, this relatively significant error occurred at one grid cell because of an anomalous wildfire (Pioneer wildfire in Idaho from July to September of 2016). Prior to the onset of the Pioneer wildfire and after the wildfire was distinguished, PM<sub>2.5</sub> returned to normal levels with respect to the *orig* simulation for *FX03* cases. ~~Y-limits~~Regardless, total accumulated values did not exceed 0.044 μg m<sup>-3</sup>, 0.34 ppbV, and 0.054 ppbV for PM<sub>2.5</sub>, O<sub>3</sub>, and NH<sub>3</sub> respectively). ~~Since errors associated with Fig. 7–9 are and by~~ predominately low magnitudes small, (maximum absolute bias), ~~in Fig. 6–8. Therefore, relatively large significant error (similar to the discrepancies in bias for PM<sub>2.5</sub> for the *FX03* cases)~~ is associated with brief spikes of certain species within and around source regions.

The final aspect of this evaluation explores differences aspects of important deposition species-rates using ~~boxplots~~bar plots which depict the sum of hourly absolute differences (for all cells across the domain) between the *orig* simulation and the altered simulations and cases (minimum, 25<sup>th</sup> percentile, median, 75<sup>th</sup> percentile, and maximum) of hourly, spatially averaged r, BIAS, NMB, and RMSE for all grid-to grid-pairs for deposition rates with respect to the *orig*-case. ~~Boxplots~~Bar plots



Range	$1.397 \times 10^{-4}$	$1.845 \times 10^{-3}$	$5.650 \times 10^{-6}$	$4.621 \times 10^{-5}$
Case	Bias	NMB (%)	r	RMSE
<u>PM<sub>2.5</sub> (<math>\mu\text{g m}^{-3}</math>)</u>	<u>-0.02828948</u>	<u>-0.37369379</u>	<u>0.53041275</u>	<u>5.01579136</u>
<u>MAD8 O<sub>3</sub> (ppb)</u>	<u>-1.70888518</u>	<u>-4.07590175</u>	<u>0.76393761</u>	<u>7.93497772</u>
<u>NH<sub>3</sub> (<math>\mu\text{g m}^{-3}</math>)</u>	<u>-0.42796669</u>	<u>-35.05920328</u>	<u>0.51400293</u>	<u>1.28576807</u>

295 Table 4: Annual bulk statistical metrics for all grid-point pairs for MAD8 O<sub>3</sub> (ppb) binned by simulation or case (row).

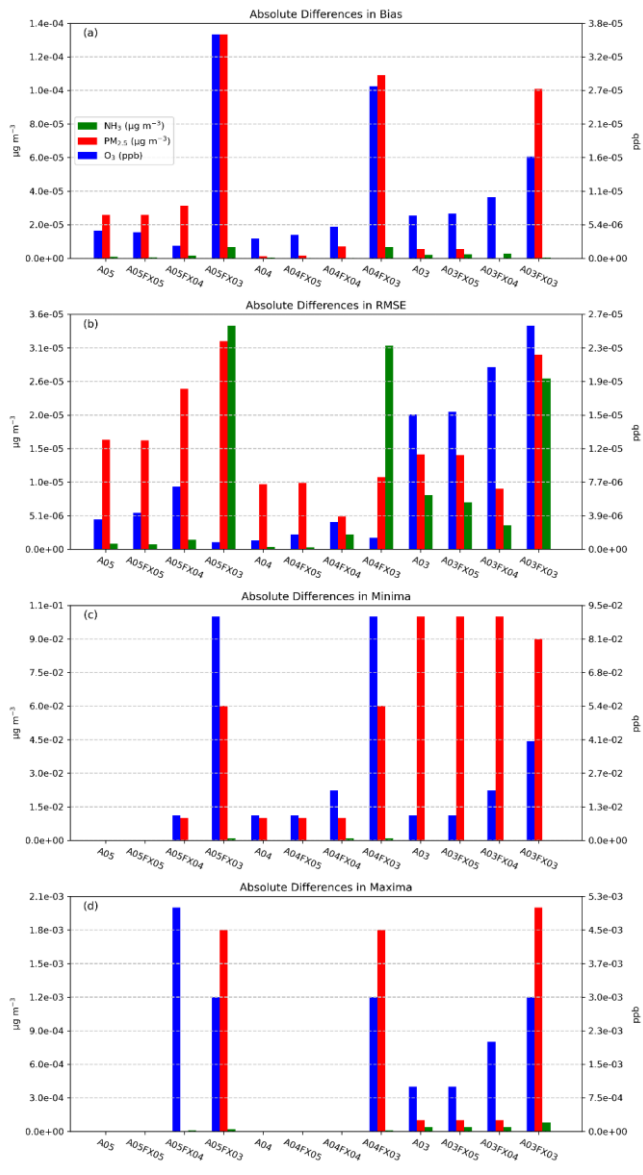
Case	Bias	NMB (%)	r	RMSE
orig	-1.70888518	-4.07590175	0.76393761	7.93497772
A05FX05	-1.70888101	-4.07589180	0.76393721	7.93498192
A05FX04	-1.70888319	-4.07589700	0.76393702	7.93498491
A05FX03	-1.70884936	-4.07581631	0.76393705	7.93497690
A05	-1.70888073	-4.07589112	0.76393725	7.93498117
A04FX05	-1.70888893	-4.07591070	0.76393754	7.93497943
A04FX04	-1.70889025	-4.07591383	0.76393745	7.93498084
A04FX03	-1.70885773	-4.07583627	0.76393726	7.93497642
A04	-1.70888837	-4.07590935	0.76393758	7.93497873
A03FX05	-1.70889237	-4.07591889	0.76393656	7.93499351
A03FX04	-1.70889496	-4.07592507	0.76393625	7.93499862
A03FX03	-1.70886892	-4.07586296	0.76393549	7.93500341
A03	-1.70889202	-4.07591806	0.76393658	7.93499319
Range	$4.560 \times 10^{-5}$	$1.088 \times 10^{-4}$	$2.120 \times 10^{-6}$	$2.699 \times 10^{-5}$

Table 5: Annual bulk statistical metrics for all grid-point pairs for daily averaged NH<sub>3</sub> ( $\mu\text{g m}^{-3}$ ) binned by simulation or case (row).

Case	Bias	NMB (%)	r	RMSE
orig	-0.42796669	-35.05920328	0.51400293	1.28576807
A05FX05	-0.42796733	-35.05925543	0.51400262	1.28576885
A05FX04	-0.42796814	-35.0593213	0.51400369	1.28576660
A05FX03	-0.42795978	-35.05863723	0.51399115	1.28580217
A05	-0.42796762	-35.05927875	0.51400259	1.28576893
A04FX05	-0.42796643	-35.0591816	0.51400300	1.28576777
A04FX04	-0.42796650	-35.05918764	0.51400269	1.28577030
A04FX03	-0.42796002	-35.05865625	0.51399133	1.28579903
A04	-0.42796635	-35.05917526	0.51400305	1.28576768
A03FX05	-0.42796899	-35.0593916	0.51399920	1.28577519
A03FX04	-0.42796939	-35.05942449	0.51400001	1.28577173
A03FX03	-0.42796703	-35.05923092	0.51398972	1.28579406
A03	-0.42796888	-35.05938233	0.51399862	1.28577635

**Range**       $9.610 \times 10^{-6}$        $7.873 \times 10^{-4}$        $4.397 \times 10^{-5}$        $3.557 \times 10^{-5}$

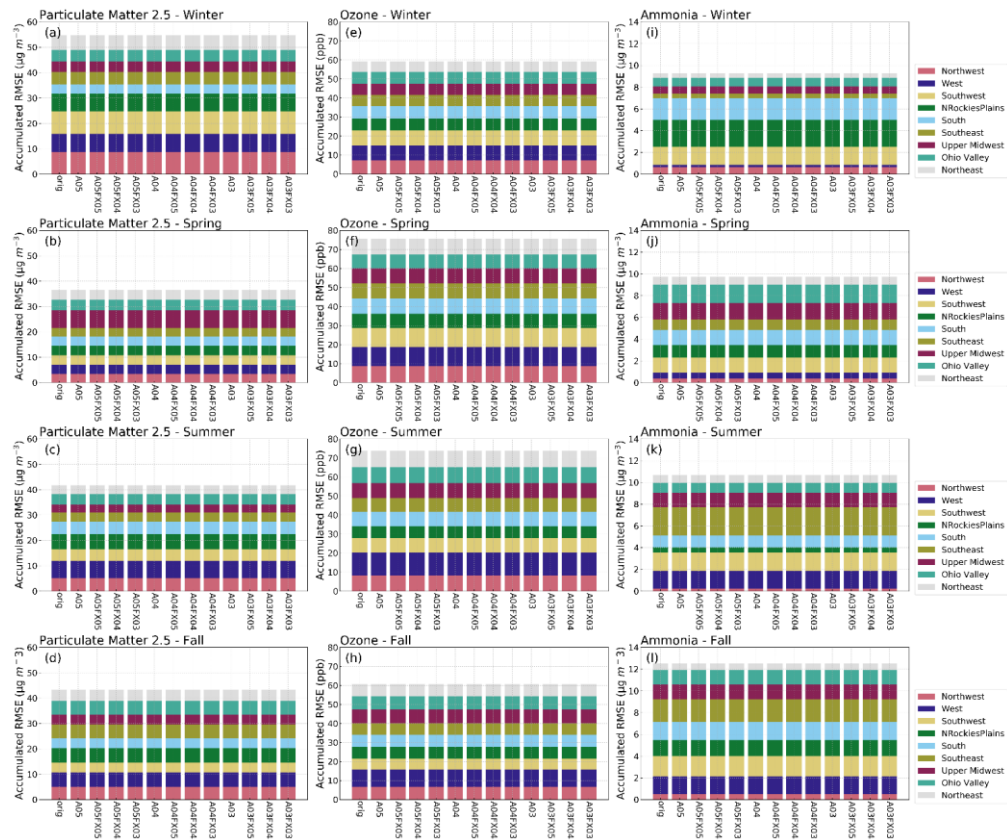
---





300

**Figure 4:** Absolute differences in bulk statistical metrics for daily PM<sub>2.5</sub>, MDA8 O<sub>3</sub>, and two-week averaged NH<sub>3</sub> between the *orig* simulation and the altered simulations and cases. Bulk statistical metrics were calculated for all model-observation pairs at in-situ stations.



305

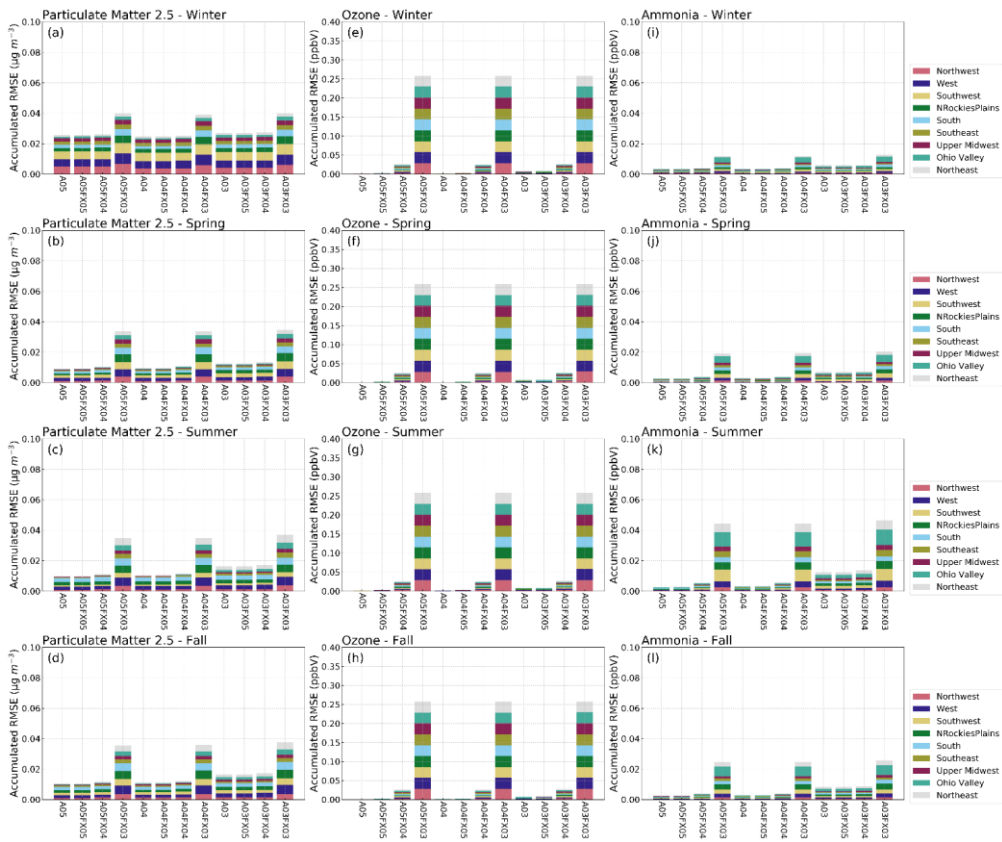
**Figure 45:** Stacked bar plots of RMSE (y-axis) stratified by region (color), simulation and case (x-axis), and season (subplot) for daily PM<sub>2.5</sub>, MDA8 O<sub>3</sub>, and daily NH<sub>3</sub> two-week averaged NH<sub>3</sub> calculated from in situ observation.

Formatted: Subscript

**Table 6:** Maximum and minimum biases (modeled—observation) for all simulations and cases (row) by variable (column) throughout 2016 utilizing in-situ observations.

Case	PM <sub>2.5</sub> (μg m <sup>-3</sup> )		Ozone (ppb)		Ammonia (μg m <sup>-3</sup> )	
	Max.	Min.	Max.	Min.	Max.	Min.

<b>orig</b>	511.6467	-161.4475	139.835	-80.685	11.3	-7.64904
<b>A05FX05</b>	511.6467	-161.4475	139.835	-80.685	11.3	-7.64904
<b>A05FX04</b>	511.6567	-161.4475	139.825	-80.68	11.3	-7.64903
<b>A05FX03</b>	511.5867	-161.4457	139.745	-80.682	11.301	-7.64906
<b>A05</b>	511.6467	-161.4475	139.835	-80.685	11.3	-7.64904
<b>A04FX05</b>	511.6367	-161.4475	139.845	-80.685	11.3	-7.64904
<b>A04FX04</b>	511.6367	-161.4475	139.855	-80.685	11.301	-7.64904
<b>A04FX03</b>	511.5867	-161.4457	139.745	-80.682	11.301	-7.64905
<b>A04</b>	511.6367	-161.4475	139.845	-80.685	11.3	-7.64904
<b>A03FX05</b>	511.7467	-161.4474	139.845	-80.684	11.3	-7.64908
<b>A03FX04</b>	511.7467	-161.4474	139.855	-80.683	11.3	-7.64908
<b>A03FX03</b>	511.7367	-161.4455	139.875	-80.682	11.3	-7.64912
<b>A03</b>	511.7467	-161.4474	139.845	-80.684	11.3	-7.64908
<b>Range</b>	0.16	0.002	0.13	0.005	0.001	$9.00 \times 10^{-5}$



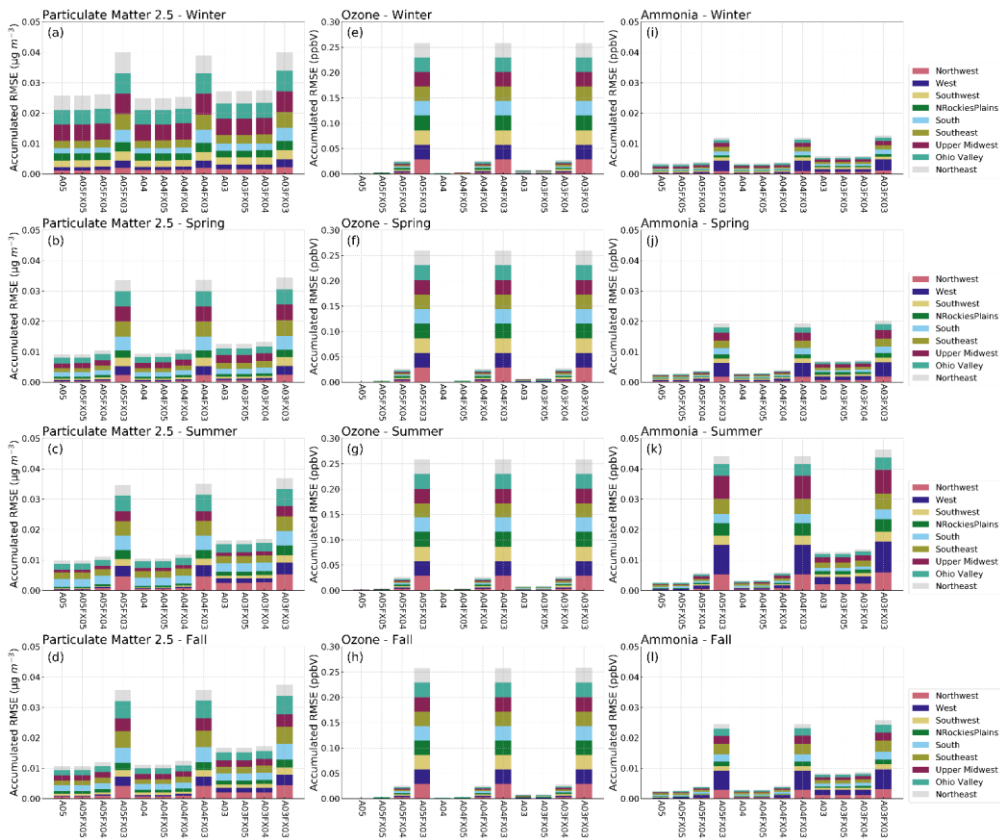
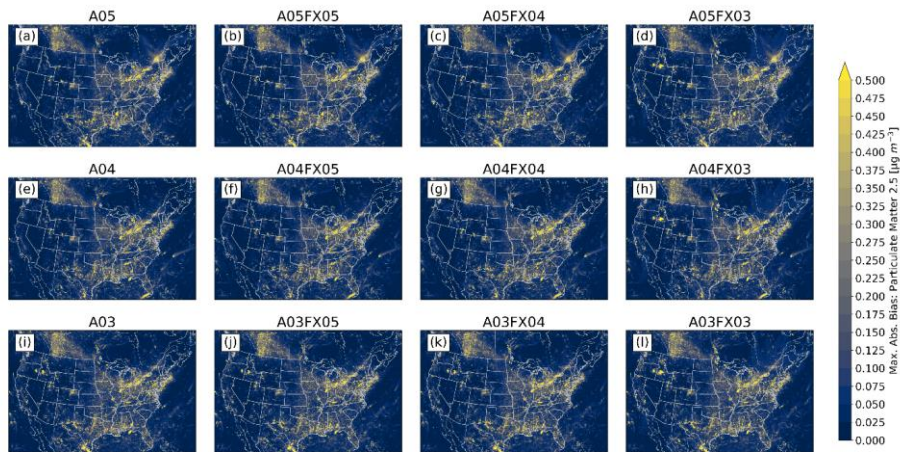
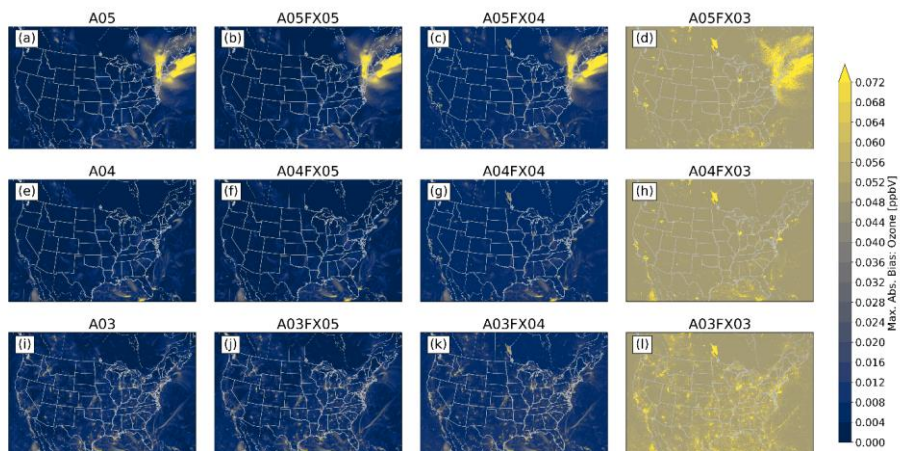


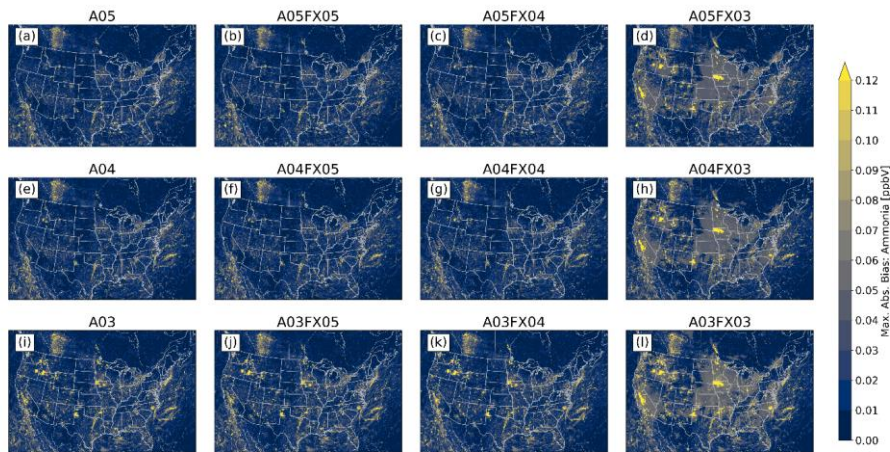
Figure 56: Stacked bar plots of RMSE (y-axis) stratified by region (color), simulation and case (x-axis), and season (subplot) for hourly PM<sub>2.5</sub>, O<sub>3</sub>, and NH<sub>3</sub> calculated from grid-grid pairs with respect to the *orig* simulation.



315 **Figure 67:** Maximum absolute bias (versus the *orig* simulation) for PM<sub>2.5</sub> calculated from hourly output for all simulations and cases.



**Figure 78:** Maximum absolute bias (versus the *orig* simulation) for O<sub>3</sub> calculated from hourly output for all simulations and cases.



320 **Figure 89:** Maximum absolute bias (versus the *orig* simulation) for NH<sub>3</sub> calculated from hourly output for all simulations and cases.

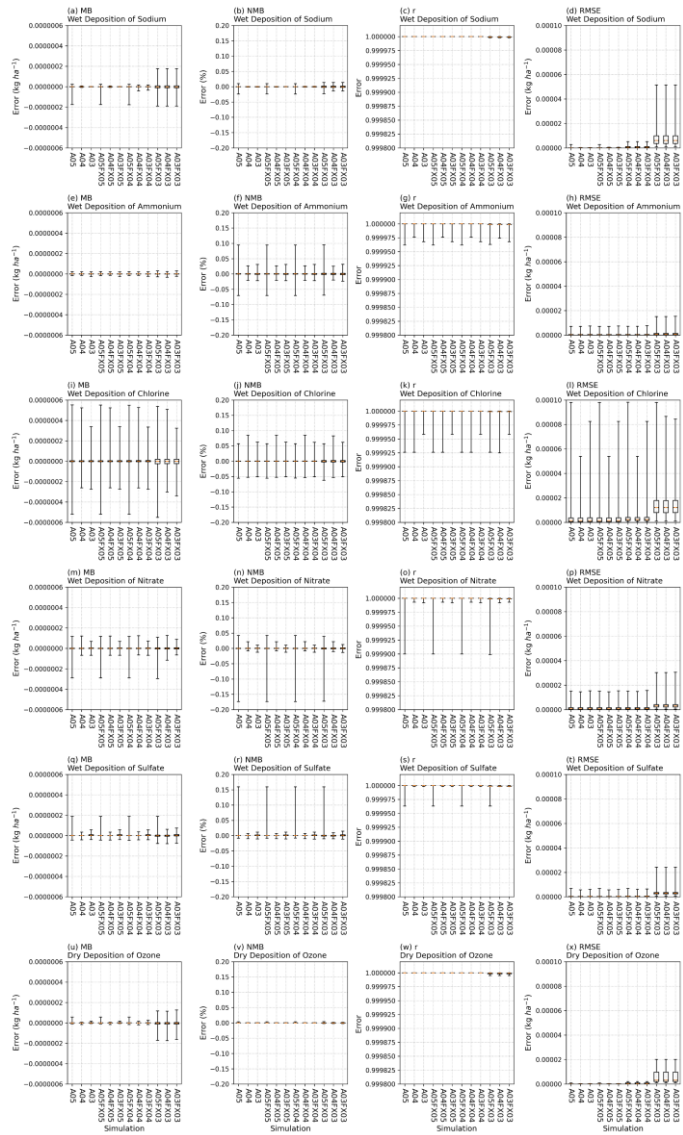
**Table 74:** Maximum and Minimum biases (*orig*—altered - *orig*) calculated from hourly CMAQ output for all simulations and cases with respect to the *orig* simulation across all grid cells

Formatted: Font: Italic

Case	PM <sub>2.5</sub> (μg m <sup>-3</sup> )		Ozone (ppbV)		Ammonia (ppbV)	
	Max.	Min.	Max.	Min.	Max.	Min.
A05FX05	4.40819836	-4.69252777	0.260878	-0.08337	0.893507	-0.61453
A05FX04	4.40777397	-4.69240379	0.263882	-0.08437	0.893806	-4.01074
A05FX03	51.17382812	-9.62011719	0.499962	-0.50085	19.64355	-4.86621
A05	4.40821075	-4.69258881	0.260483	-0.08343	0.893517	-0.61455
A04FX05	4.99303246	-4.70221233	0.136284	-0.16548	0.875244	-1.14815
A04FX04	4.99263382	-4.70223236	0.136154	-0.16448	1.275146	-4.01074
A04FX03	51.1640625	-9.51953125	0.503494	-0.50282	19.64355	-5.02832
A04	4.99302673	-4.70224953	0.13604	-0.16512	0.867432	-1.14854
A03FX05	11.09228516	-6.66992188	0.223785	-0.22272	4.146118	-7.44141
A03FX04	11.54589844	-10.265625	0.225784	-0.22272	4.446045	-7.0415
A03FX03	41.18359375	-9.46972656	0.562561	-0.59249	19.64355	-10.3923
A03	11.17675781	-7.01953125	0.224041	-0.22235	4.187866	-7.47461
<b>Range</b>	<b>46.76605415</b>	<b>5.57322121</b>	<b>0.426521</b>	<b>0.509121</b>	<b>18.77612</b>	<b>9.777804</b>

Formatted Table





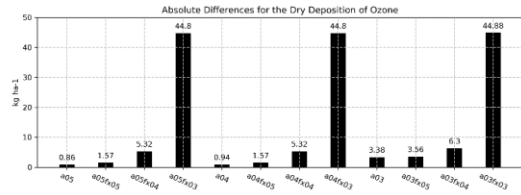
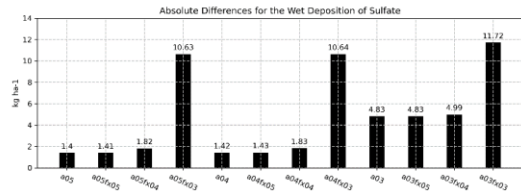
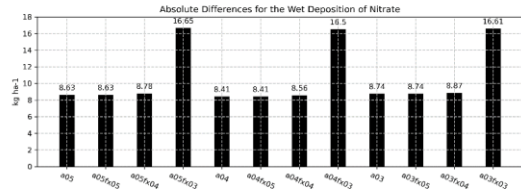
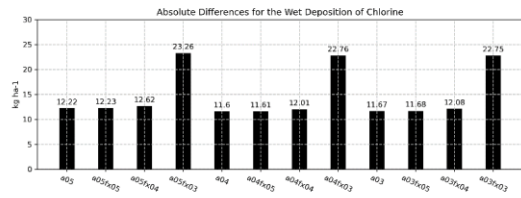
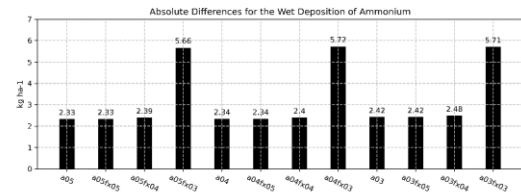
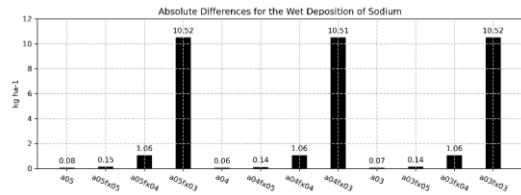




**Figure 910: Total absolute bias difference between the *orig* simulation and the altered cases and simulations by deposition rate** Boxplots of hourly and spatially averaged statistics (column) for multiple deposition species (row) throughout 2016 utilizing hourly output.

#### 330 4. Conclusion

We have demonstrated that altering data by keeping a specified number of significant digits in terms of emission input and/or simulated output, increased compression efficiency based on two different, popular compression utilities (gzip and bzip2). For emission data, bzip2 performed far better than gzip and provided compression reduction, on average, by 6 %, 25 %, and 48 % for emission data, and 19 %, 47 %, and 69 % for output data for the *A05*, *A04*, and *A03* cases respectively, compared to the *orig* case. In terms of daily simulation runtime for the entire simulation year, the *A05*, *A04* and *A03* simulations consistently were faster than the *orig* simulation in an undedicated HPC system for most simulation days.

As for accuracy, results for all studied simulations, either with altered altered-precision emission only, or with altered altered-precision emission plus altered altered-precision output, produced numerically insignificant differences. For example, the maximum absolute, bulk statistical difference between the *orig* simulation and the altered cases and simulations for daily  $PM_{2.5}$ , MDA8  $O_3$ , and two-week averaged  $NH_3$  did not exceed  $1.4 \times 10^{-4}$ ,  $3.6 \times 10^{-5}$ ,  $1.1 \times 10^{-1}$ , and  $5.3 \times 10^{-3} \mu g m^{-3}$  or ppb for bias, RMSE, minima, and maxima, respectively the bulk statistic ranges of NMB for daily  $PM_{2.5}$ , MDA8  $O_3$ , and  $NH_3$ , compared to all cases and simulations at in-situ locations, are  $1.845 \times 10^{-3} \%$ ,  $1.088 \times 10^{-4} \%$ , and  $7.873 \times 10^{-4} \%$ . Similarly, small range in values is replicated for all other bulk statistical metrics such as MB, r, and RMSE. Results stratified by region and season mimic are similar to those for bulk statistics. Based on the in-situ in-situ evaluation, simulation performance is very similar amongst all cases, with visible differences for the *A03* simulation and the *FX03* cases in which error is spatially detected in Fig. 67-89.

Statistical inconsistencies arise when comparing grid-grid values of hourly  $PM_{2.5}$ ,  $O_3$ , and  $NH_3$  versus the *orig* simulation. Results indicate that similarities amongst the *orig* simulation decreases with fewer significant digit simulations and cases when analyzing the stacked and stratified (region and season) RMSE bar plot (Fig. 56). More specifically, performance with respect to the *orig* simulation is worse for the *A03* simulation and as well, for the *FX03* cases. Such discrepancies do not occur consistently based on results provided by boxplots-bar plots of statistical metrics of deposition rates (Fig. 910). Instead, errors appear to be confined to source regions at specific instances based on the maximum absolute (hourly) error spatial plots with respect to the *orig* simulation (Fig. 67-89).

In summary, altering datasets by truncation to retain fewer significant digits significantly improved data compression and slightly improved runtime. Based on the thorough, yet spatially limited, in situ evaluation, this study has shown this proposed technique did not compromise model performance-accuracy based on an evaluation of simulations and cases at in situ locations compared to current air quality thresholds for daily  $PM_{2.5}$ , MDA8  $O_3$ , and daily  $NH_3$  two-week averaged  $NH_3$ . These results show the optimal benefit of altering CMAQ input data by keeping five-three significant digits then subsequently but strongly suggest keeping four significant digits and keeping three significant digits can be considered for

Formatted: Subscript

360 [CMAQ output data](#). In addition, this proposed technique could be beneficial for groups that perform complex air quality modeling and want to improve disk space management while negligibly impacting the [quality-accuracy](#) of the simulations. Based on the success of this study, we propose testing these techniques on the rest of CMAQ input files such as initial conditions, boundary conditions and meteorological data to determine the viability of these techniques to more adeptly manage disk space without compromising the quality of the CMAQ simulations used for research and to develop air quality management strategies.

#### Code and data availability

The source code of the tool to alter data by keeping a specific number of significant digits and a run script which includes usage instructions, for this tool, is available from DOI: 10.5281/zenodo.6620983. CMAQ 5.3.1 is available at <https://www.epa.gov/cmaq/access-cmaq-source-code>. Original, [unaltered/unaltered](#) CMAQ input data for this study is available at <https://dataverse.unc.edu/dataset.xhtml?persistentId=doi:10.15139/S3/MHNUNE>. Original, [unaltered/unaltered](#) CMAQ input data for this study from 1/1 – 1/5/2016 is available at DOI: 10.5281/zenodo.6624164.

#### Author contribution

MW conducted the runs, performed data analysis, created graphics, and wrote the first draft of the manuscript and worked with DCW to improve it. DCW originated and oversaw this work, coded the tool to alter data by keeping a specific number of significant digits, created scripts to run the entire experiment, outlined the first draft of the manuscript, and contributed to writing and improving the manuscript.

#### Competing interests

The authors declare that they have no conflict of interest.

380 **Disclaimer:** The views expressed in this paper are those of the authors and do not necessarily reflect the view, or policies, of the U.S. EPA.

#### References

385 [Appel, K. W., Bash, J. O., Fahey, K. M., Foley, K. M., Gilliam, R. C., Hogrefe, C., Hutzell, W. T., Kang, D., Mathur, R., Murphy, B. N., Napelenok, S. L., Nolte, C. G., Pleim, J. E., Pouliot, G. A., Pye, H. O. T., Ran, L., Roselle, S. J., Sarwar, G., Schwede, D. B., Sidi, F. I., Spero, T. L., and Wong, D. C.: The Community Multiscale Air Quality \(CMAQ\) model versions](#)

[5.3 and 5.3.1: system updates and evaluation, Geosci. Model Dev., 14, 2867–2897, https://doi.org/10.5194/gmd-14-2867-2021, 2021.](https://doi.org/10.5194/gmd-14-2867-2021)

Burrows M. and Wheeler D. J.: A Block Sorting Data Compression Algorithm, Tech. report, Digital Systems Research Center, Digital Equipment Corporation, Palo Alto, CA, <http://citeseerx.ist.psu.edu/viewdoc/summary?doi=10.1.1.37.6774>, 1994.

Byun, D. and Schere, K. L.: Review of the governing equations, computational algorithms, and other components of the Models-3 Community Multiscale Air Quality (CMAQ) modeling system, *Appl. Mech. Rev.*, 59(2), 51-77, <https://doi.org/10.1115/1.2128636>, 2006.

Deutsch, L. P.: DEFLATE compressed data format specification version 1.3, Tech. Rep. IETF RFC1951, Internet Engineering Task Force, Menlo Park, CA, USA, <https://doi.org/10.17487/RFC1951>, 1996.

Huffman, D. A.: A method for the construction of minimum redundancy codes, *Proceedings of the IRE*, vol. 40, no. 9, Sept. 1952, pp. 1098–1101, doi: 10.1109/JRPROC.1952.273898, 1952.

Kouznetsov, R.: A note on precision-preserving compression of scientific data, *Geoscientific Model Development*, 14, 377–389, <https://doi.org/10.5194/gmd-14-377-2021>, 2021.

Kryukov, K., Ueda, M. T., Nakagawa, S., and Imanishi, T.: Sequence Compression Benchmark (SCB) database—A comprehensive evaluation of reference-free compressors for FASTA-formatted sequences, *GigaScience*, Volume 9, Issue 7, gaa072, <https://doi.org/10.1093/gigascience/gaa072>, 2020.

United States Environmental Protection Agency: The Community Multiscale Air Quality Model version 5.3.1 [Software], [doi.org/10.5281/zenodo.3585898](https://doi.org/10.5281/zenodo.3585898), 2019.

Zender, C. S.: Bit Grooming: statistically accurate precision-preserving quantization with compression, evaluated in the netCDF Operators (NCO, v4.4.8+), *Geosci. Model Dev.*, 9, 3199–3211, <https://doi.org/10.5194/gmd-9-3199-2016>, 2016.

Ziv, J. and Lempel, A.: A universal algorithm for sequential data compression, *IEEE Transactions on Information Theory*, vol. 23, no. 3, 337–343, <https://doi.org/10.1109/TIT.1977.1055714>, 1977.